Layered Manufacturing of Nanocrystalline Copper Parts Using Pulse Jet Electrodeposition and its Mechanical Properties

*Hui Fan[1, *], Yangpei Zhao[2], Jie Jiang[3], Shankui Wang[1], Zhijing Li[1]*

[1] School of Mechanical and Electrical Engineering, Jiangsu Normal University, Xuzhou, 221116, China
[2] Jiangsu Vocational Institute of Architectural Technology, Xuzhou, 221116, China
[3] Jiangsu Key Laboratory of 3D Printing Equipment and Application Technology, Nantong Institute of Technology, Nantong, 226002, China
[*]E-mail: xzfanhui@163.com

A new type of layered manufacturing technology that combines the jet electrodeposition method and a rapid prototyping concept is presented. The manufacturing method adopts multilayer scanning electrodeposition using an electrolyte jet to fabricate a micro-metallic part with a nanocrystalline microstructure, which simplifies three-dimensional processing. The research results showed that key parameters, including the current density, applied voltage, nozzle diameter and jet speed, impacted the forming process and deposition quality. The effective current density was observed to reach 350 A/dm^2, at which point nanocrystalline grains with sizes from 30-50 nm were obtained. It was found that the application of an optimized applied voltage, nozzle diameter, current density and jet velocity increased the forming speed and improved the mechanical performance of the finished parts. A group of nanocrystalline copper parts with a good shape and mechanical properties was produced using optimized parameters with the jet electrodeposition method.

1. INTRODUCTION

Rapid prototyping manufacturing (RPM) has attracted widespread attention for the manufacturing of complex-shaped parts. RPM is based on the principle of additive manufacturing; the whole manufacturing process for a three-dimensional part can be transformed to a series of layer-by-layer planar processes, thereby reducing processing difficulties [1-3]. At present, RPM technologies mainly include stereolithography (SLA), fused deposition manufacturing (FDM) and selective laser sintering (SLS) [4-7]. Although these technologies have been extensively employed in the fabrication of complex parts, they have been rarely applied to the fabrication of small metallic parts [5]. Researchers

are also exploring other fabrication methods for small metal parts, including electrical discharge precision machining, LIGA and quasi-LIGA technologies. However, they are generally expensive, complicated and have long preparation times [8, 9].

Electrodeposition is a common process technology that produces metallic parts based on electrochemical reactions on a cathode. It is known for its cost effectiveness, high manufacturing accuracy, low energy consumption and low thermal residual stress compared with those for laser sintering, stereolithography and other high-energy field process technologies [10-18]. Among various electrodeposition technologies, jet electrodeposition has become an emerging technology in recent years [19-26], which sprays a high-speed electrolyte jet that contains a high-concentration of metal anode ions onto a cathode surface, as shown in Figure 1. Compared with that of traditional electrodeposition, this method is able to provide a much higher current density and produce a nanocrystalline microstructure in finished parts [27-30], and it possesses the advantages of high current efficiency, grain refinement and a dense material microstructure. In the last decade, Jet electrodeposition technology has attracted widespread attention. Shen and Wang et al [31] employed jet electrodeposition in a rotating way to prepare an NdFeB coating on the substrate of stainless, effectively improve the uniformity and compactness of coatings and enhance the corrosion resistance. Fan and Zhao [14] produced a Cu-Al_2O_3 nanocompound coating via jet electrodeposition and the mechanical performance was effectively strengthened. However, there is lack of using jet electrodeposition to develop laminated manufacturing technology for micro metal devices. Few research on the influence of jet electrodeposition parameters on the micro-nano manufacturing process has been conducted.
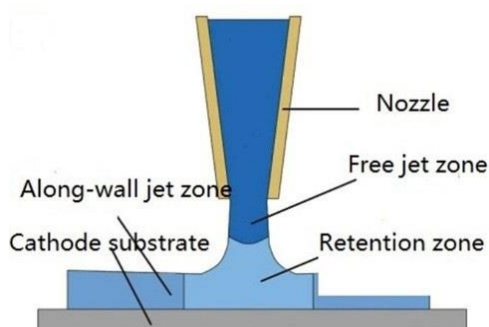

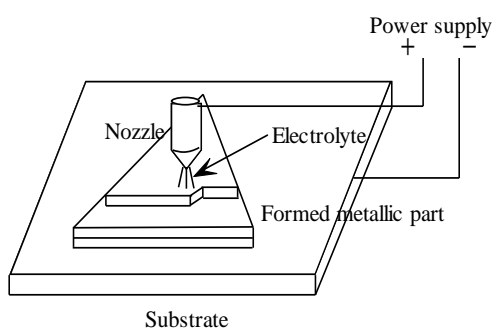**Figure 1.** Schematic diagram for a typical jet electrodeposition process

Figure 2. Schematic diagram of jet electrodeposition for rapid prototyping

Based on the above problems, the main innovation of this research is to combine jet electrodeposition technology and the typical layered manufacturing concept of RPM to develop a new method of direct rapid prototyping of metal parts (shown in Figure 2). It can economically and easily prepare three-dimensional small-sized nanocrystalline metal parts with good mechanical properties. The influence of jet electrodeposition process parameters on machining processes, such as surface quality, process speed and mechanical properties of finished parts, are studied herein. A group of nanocrystalline copper parts with different shapes and thicknesses are formed with jet electrodeposition.

2. EXPERIMENTAL PROCEDURES

2.1 Experimental apparatus and processing principles

The experiments are completed on a jet-electrodeposition experimental platform, as shown in Figure 3a. The platform is mainly composed of a CNC platform, a nozzle and its lifting mechanism, an electrolyte circulation and speed control system, a power supply, and a temperature control device. According to the input NC code instructions, the cathode plate can be directionally moved in the XY plane, and the Z axis can be controlled to move up and down to position the nozzle, thereby achieving comprehensive control of the jet distance and scanning layers. In addition, the current density, electrolyte jet velocity and scanning speed also ensure controllability. For rapid prototyping of parts by jet electrodeposition, a three-dimensional model of the part is first generated by a CAD system, and then it is output in STL file format. Afterwards, with the use of a special layered slicing software, the process system derives the cross-sectional shape of each layer of the part model and exports the planar scanning trajectory of the nozzle (see Figure 3b). Then, the nozzle is guided to execute two-dimensional planar electrodeposition according to the scanning trajectory. After completing one deposition layer, the nozzle automatically increases the layer thickness and starts the deposition for the next layer. In this way, the layers are superimposed to form a three-dimensional part.
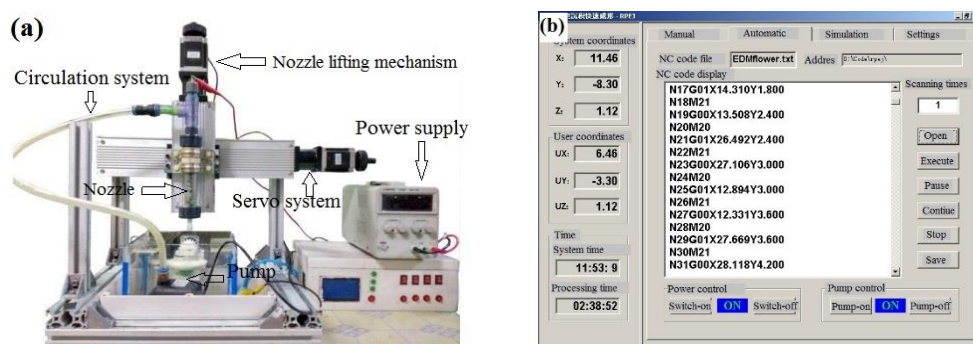

Figure 3. Jet electrodeposition system (a) experimental apparatus and (b) control software interface

A copper rod was installed inside the nozzle cavity and acted as the anode. The cathode substrate comprised a 304 stainless steel sheet with dimensions of $100 \times 100 \times 2$ mm. The electrolyte contained 250 g/l $CuSO_4 \cdot 5H_2O$ (Nanjing regent; 99% purities) and 50 g/l H_2SO_4 (Nanjing regent; 98% purities). The

pH value of the electrolyte was maintained at 4 by adding dilute sulfuric acid or NaOH. Table 1 shows the other experimental conditions.

Table 1. Jet electrodeposition process parameters

Deposition parameter	Value
Nozzle diameter	1-5 mm
Jet distance	3 mm
Electrolyte jet velocity	2-10 m/s
Scanning rate	1000 mm/min
Current density (Pulse)	150-450 A/dm^2
Pulse frequency	12000 Hz
Duty ratio	1:3
Deposit thickness	500-1000 μm
Temperature	50 ℃

The morphology and crystal structure of the coating were analysed by scanning electron microscopy (SEM). The microhardness of the finished parts was tested on an HXS-1000a Vickers microhardness tester (produced by Shanghai Microscope, China). The tensile strength of the composite coating was measured on a thin film material testing machine (Sansi, China).

3. RESULTS AND DISCUSSION

3.1 Effect of the current density on the deposit material morphology

The growth morphology of the deposit surface determines the overall quality and interlayer bonding of the shaped parts. Figure 4 shows the deposit morphology over the current density range from 150-450 A/dm^2. When the current density is 150 A/dm^2, a cell-like particle growth morphology appears on the deposition surface, as shown in Figure 4a. When the current density increases to 350 A/dm^2, the deposit layer tends to be flat, with few observed nodules or defects. In the magnified area in the upper right corner of Figure 4b, a number of fine nanocrystalline particles with sizes from approximately 30-50 nm can be found. As the current density exceeds 300 A/dm^2, cell-like particles reappear, and at 450 A/dm^2, the deposit surface becomes coarse and isolated, and the particles are no longer connected. It can be concluded that the critical effective current density is 350 A/dm^2 under these experimental conditions. When the current density is less than this value, the deposit layer becomes smooth and flat with refined nanocrystalline grains. Once the current density is greater than this value, the deposit surface gradually deteriorates, cell-like particle growth occurs and uniform dendrite growth begins. In the literatures [31, 32], Dong and Qiao et al also pointed that if excessive current density was applied, the hydrogen precipitation would become serious and led to internal stress, with the coating becoming brittle in lack plasticity. Simultaneously, the current experimental results proves that with the increase of current

density, cellular bulges and dendrites will indeed become denser on the surface of the coating. The current is highly concentrated due to the tip effect, which makes the electrodeposition unable to continue. Therefore, the appropriate current density is believed the key to the parameters of jet electrodeposition.
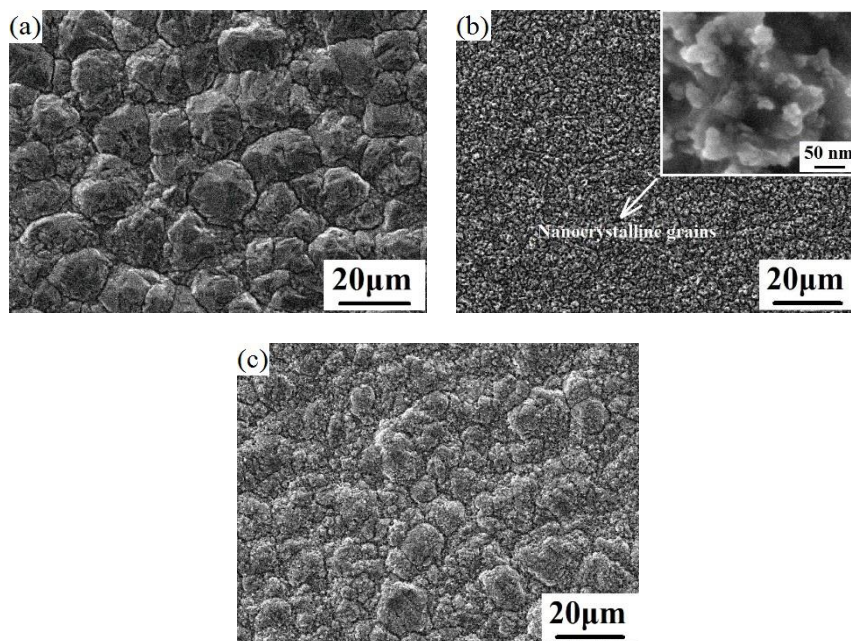

Figure 4. Morphological changes of deposit surface under the various current densities (a) 150 A/dm^2 (b) 350 A/dm^2 and (c) 450 A/dm^2 (jet velocity 10 m/s and nozzle diameter 2 mm)

3.2 Effect of the applied voltage on the current density

The current density affects the deposition quality and processing speed for each layer, as shown in Figure 4. It is of great significance to study the change in the current density during the deposition process. Figure 5 shows the relationship between the applied voltage and current density. It can be seen from the figure that the current density increases with increasing applied voltage linearly. It can also be seen that the current density in the experiment reaches 450 A/dm^2. In fact, during traditional electrodeposition, the current density usually does not exceed 10 A/dm^2, which results in a slower electrodeposition rate. During jet electrodeposition, a high current density can be obtained because a high concentration of metallic ions in the electrolyte is continuously sprayed towards the cathode surface in a forced manner at high speed, which can quickly replenish the amount of metal ions on the cathode surface and greatly improve the material migration rate [31-37]. At the same time, the electrolyte not only mechanically activates the deposited layer but also greatly reduces the diffusion layer and the concentration polarization, thus greatly increasing the limit current density and achieving high-speed electrodeposition. Xia and Jiang [38, 39] used the jet electrodeposition method to produce Ni-SiC composites with current densities as high as 100-120 A/dm^2, which is 20 times that of traditional Ni electrodeposition. Also, according to the literature [40, 41], Liu and Fan et al also verified the linear relationship between the current and the voltage of jet electrodeposition with the maximum current density 160 A/dm^2. It was also revealed if the voltage exceeded 30V, the coating surface would be

scorched. The experimental result in literature [40] is basically coincide with this study, but its highest applied current density is only 120 A/dm^2, compared with the highest current density in this research attaining 450 A/dm^2. This is because different deposited metal and a higher jet velocity are used in this research.
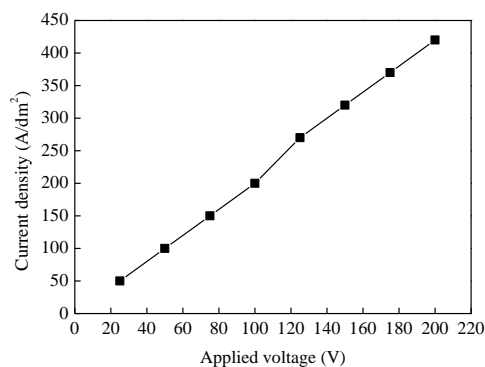

Figure 5. Influence of applied voltage on the current density at (jet velocity 10 m/s and nozzle diameter 2 mm)

3.3 The effect of the applied voltage on the electrodeposition rate

Figure 6 shows the effect of the applied voltage on the electrodeposition rate. It can be seen in the figure that for an applied voltage from 20-200 V, the electrodeposition rate shows a proportional relationship with the applied voltage. In addition, it can also be seen that when the applied voltage is less than 150 V, the electrodeposition rate has a good linear relationship with an increase in the applied voltage. However, when the applied voltage is greater than 145 V, the slope of the line is obviously increased, indicating that the electrodeposition rate highly increases. This is mainly because when the voltage is greater than 145 V, the current density nearly reaches 350 A/dm^2, which is a critical value, as previously mentioned. As the voltage increases, the deposit surface becomes increasingly worse and forms many obvious cell-like particles that attract a more concentrated current. Therefore, the current concentration suddenly increases the electrodeposition process.
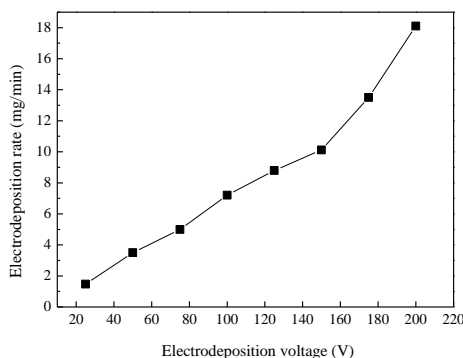

Figure 6. Effect of the applied voltage on the electrodeposition rate at (current density 350 A/dm^2, jet velocity 10 m/s and nozzle diameter 2 mm)

Although appropriately increasing the applied voltage increases the deposition rate, an over-high voltage also increases the current density and promotes the formation of cellular bulges on the surface of the deposition layer, which worsens the deposition quality, as shown in Figure 4. Also Tian et al [42] proposed that nodule and dendrite derivatives would appear on the surface of the deposition layer after the jet electrodeposition voltage exceeded 80V. The reason lies in the uneven growth of the deposition layer surface caused by high voltage, resulting in agglomeration effect and worsening the finished surface flatness and quality.

3.4 Effect of the nozzle diameter on the electrodeposition rate

Figure 7 shows the effects of the nozzle diameter on the electrodeposition rate and the electrodeposition spot size. It can be seen that under the same applied voltage, the size of the nozzle diameter has a significant effect on the electrodeposition rate. At a nozzle diameter of 5 mm, the electrodeposition rate is approximately 10 times that of a nozzle diameter of 1 mm. Actually, under the same applied voltage and jet velocity, the average current density remains unchanged, and an increase in the nozzle size correspondingly increases the deposition spot (the area on the cathode surface where electrodeposition occurs under the nozzle), thereby increasing the electrodeposition rate and the deposition efficiency. However, the nozzle diameter cannot be excessively increased because an overly large nozzle size increases the deposition spot too much and influences the forming accuracy. Additionally, as shown in Figure 7, the deposition spot increases linearly with increasing nozzle diameter, and the spot size is approximately twice the nozzle diameter.
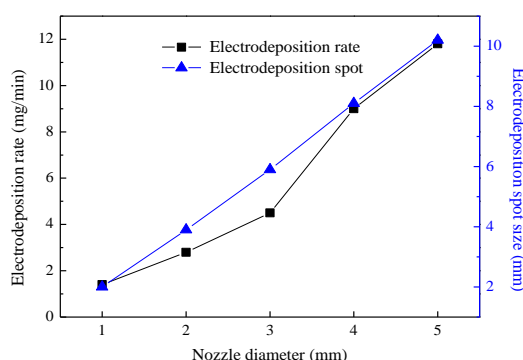

Figure 7. Effect of nozzle diameter on the electrodeposition rate and electrodeposition spot at (current density 350 A/dm^2, jet velocity 10 m/s and nozzle diameter 2 mm)

According to the literature [43], it is revealed the dense, uniform and smooth Ni-SiC nano-coating can be prepared by jet electrodeposition with appropriate nozzle diameter, which can effectively prevent the invasion of corrosion solution and make the coating have excellent corrosion resistance. When the nozzle diameter is too small or too large, there are a large number of cauliflower like coarse grains on the surface of N-SiC nano-coating prepared by jet electrodeposition, which significantly increases the contact area between corrosion solution and coating. According to the curve in this research, a small nozzle diameter leads to a small electrodeposition spot and a high dimensional forming accuracy. Therefore, the nozzle diameter should be selected reasonably for the actual situation.

3.5 Effect of the jet velocity on the electrodeposition rate

The relationship between the jet velocity and electrodeposition rate is shown in Figure 8. The electrodeposition rate has a basically linear relationship with the jet velocity, which means that the electrodeposition rate increases with an increase in the jet velocity. In addition, the curve is not very steep, indicating that an increase in electrodeposition rate is limited. In fact, an increasing jet velocity accelerates the mass transfer process of the liquid phase and shortens the time for the metal copper ions travelling to the cathode surface, which is equivalent to a decrease in the resistance of the electrolyte and an increase in the current.
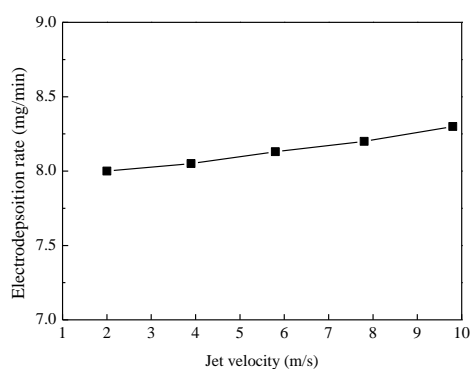

Figure 8. Effect of the jet velocity on the electrodeposition rate at (current density 350 A/dm^2 and Nozzle diameter 2 mm)

In addition, an increase in the jet velocity expands the jet column and enlarges the deposition spot, thereby accelerating the electrodeposition rate. Huang and Chen et al [44] proposed the influence factors on the deposition rate of the coating. They found the deposition rate first increased and then decreased with the increase of voltage and temperature. This is because the increase of voltage leads to the increase of current density and the increase of electrochemical polarization, which leads to the increase of deposition rate. However, compared with the applied voltage, the effect of jet velocity on the electrodeposition rate is limited. If there is a need to increase the electrodeposition rate, an increase in the applied voltage should first be adopted.

3.6 Rapid prototyping copper parts and their mechanical properties

By using the jet electrodeposition forming system, a group of metal copper parts with thicknesses of 0.5 mm were formed, as shown in Figure 9, with the following optimized experimental conditions: an applied voltage of 145 V, a current density of 350 A/dm^2, a jet velocity of 8 m/s, a nozzle scan speed of 10 mm/s, and a nozzle diameter of 1 mm. The copper parts have a clear outline with dimensional accuracy along the X and Y directions up to 10 mm ± 0.2 mm and fillet radius r < 1.5 mm.
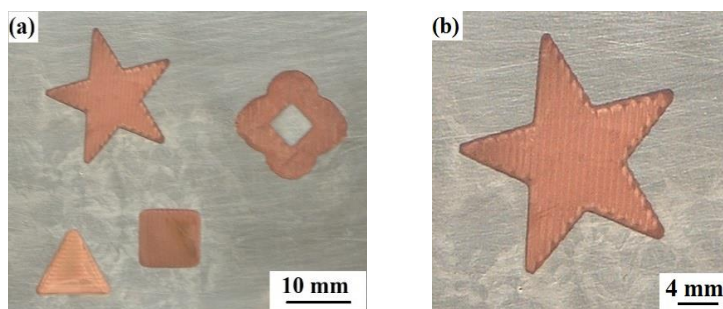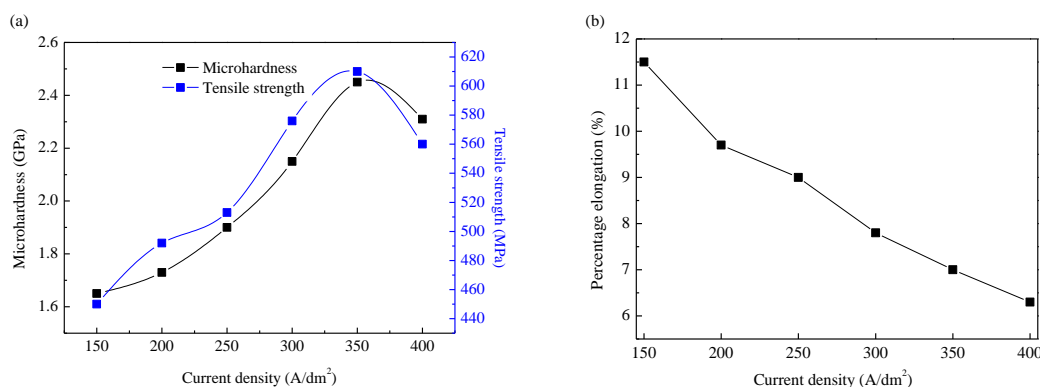
Figure 9. The formed copper parts with different shapes (a) a group of parts and (b) a magnified image of the pentagram at (current density 350 A/dm^2, jet velocity 10 m/s and nozzle diameter 2 mm)

Additionally, the formed nanocrystalline copper parts have a high strength and microhardness. The effect of the pulse current density on the mechanical properties of the deposit layer is studied. Figure 10 a shows that the microhardness and tensile strength of the deposited copper part samples increase with increasing current density, and the maximum values are 2.41 GPa and 610 MPa, respectively, at a current density of 350 A/dm^2, which is consistent with the results of the morphology comparison. The maximum tensile strength of the nanocrystalline copper is 4.5 times that of ordinary coarse-grained copper. It can also be seen in Figure 10b that the elongation of the nanocrystalline copper decreases with increasing current density. When the average current density increases from 200 A/dm^2 to 400 A/dm^2, the elongation decreases from 9.7% to 6.3%, respectively. The stress-strain curve of the nanocrystalline copper part has the same characteristics during stretching, and there is a certain strain strengthening phenomenon during the plastic deformation process, as shown in Figure 10 c. Fan and Zhao et al in literature [41] had the similar observation that when a Cu-Al$_2$O$_3$ nanocompound coating was prepared, current density in the range of 100-500 A/dm^2 could offer grain refining effect by providing nano-crystalline copper composited coating with a size between 40 and 70 nm. However, if excessive current density (more than 400 A/dm^2) was applied, it would fail to improve the surface morphology and microstructure, and even deteriorate the coating's forming quality. Therefore, appropriate current density in jet electrodeposition can not only improve the deposition quality, but also refine the grain size and improve the mechanical properties of the coating.
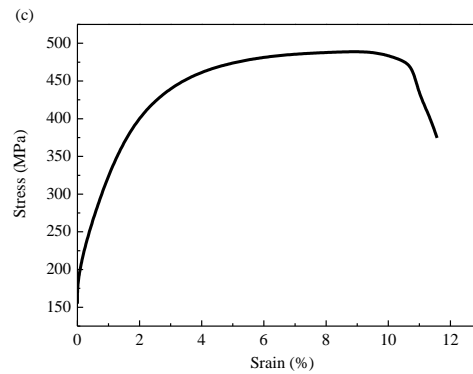
Figure 10. Mechanical properties of the formed copper parts, including the (a) microhardness and tensile strength, (b) percentage elongation and (c) stress-strain curve at (current density 350 A/dm^2, jet velocity 10 m/s and nozzle diameter 2 mm)

4. CONCLUSION

A new manufacturing technology combining the advantages of jet electrodeposition and the layered manufacturing concept of RPM was presented. The self-developed jet electrodeposition forming system can directly shape a variety of metal parts with different complex shapes and has an improved shape and size accuracy. The influence of jet electrodeposition process parameters on the machining processes was systematically studied. The highest effective current density was found to be 350 A/dm^2, which is much higher than that of traditional electrodeposition and achieved high-speed nanocrystalline copper electrodeposition. It was also found that the optimized parameter combination, including the applied voltage, current density, jet velocity and nozzle diameter, increased the forming speed and improved the mechanical performance of the finished parts.

References

1.   J. P. Kruth, M. C. Leu and T. Nakagawa. *CIRP Ann-Manuf. Technol.*, 47 (1998) 525.
2.   T. Wohlers. *Rapid Prototyping J.*, 1 (1995) 4.
3.   X. Yan and P. Gu. *Comput.-Aided Des.*, 28 (1996) 307.
4.   D. G. Coblas, A.Fatu and A. Maoui. *Proc. Inst. Mech. Eng. Part J.-J. Eng. Tribol.*, 229 (2015) 3.
5.   A. D. Lantada and P. L. Morgado. *Annu. Rev. Biomed. Eng.*, 17 (2012) 73.
6.   Z. Xuan, N. Qu and Z. Hou. *Chin. J. Aeronaut.*, 31 (2018) 1609.
7.   H. C. Tsai, B. H. Yan and F. Y. Huang. *Int. J. Mach. Tools Manuf.,* 245 (2003) 43.
8.   O.Yilmaz and M.A. Okka. *Int. J. Adv. Manuf. Technol.,* 185 (2010) 51.

9. X.L. Meng, X.Y. Fan and Y.H. Guo. *Steel Res. Int.,* 90 (2019) 1900037.
10. C. K. Yang , C. P. Cheng, C.C. Mai, A.C.Wang, J.C. Hung and B. H. Yan. *Int. J. Mach. Tools Manuf.,* 50 (2010) 1088.
11. M. Hamdi. *Int. J. Adv. Manuf. Technol.,* 76(2015) 329.
12. G. D'Urso, G. Maccarini and C. Ravasio . *Int. J. Adv. Manuf. Technol.,*72 (2014) 1287.
13. L. Li, X. T. Wei and G. M. Zheng. *Mater. Manuf. Process.,* 776 (2016) 31.
14. H. Fan, Y.P. Zhao, S.N. Cao, and Z.J. Li. *Mater. Trans.,* 60 (2019) 802.
15. N.S. Qu, K.C. Chan and D. Zhu. *Surf. Coat. Technol.,* 91 (1997) 220.
16. H. Fan, S.N. Cao, Y.P. Zhao and S.K.Wang. *Int. J. Electrochem. Sci.*, 14(2019) 8256.
17. Y.W. Yao, S.W. Yao, L. Zhang and H.Wang. *Mater. Lett.,* 61 (2007) 67.
18. D.Q. Zhao, X. Jiang, Y.X. Wang, W. Duan and L. Wang. *Appl. Surf. Sci.,* 457 (2018) 914.
19. C.J. Xiao. *Surf. Eng.,* 34 (2018) 832.
20. H. Fan, Z.J. Li, Y.P. Zhao, S.K.Wang and S.N. Cao. *Int. J. Electrochem. Sci.*, 14(2019) 3326.
21. M. Poorraeisi and A. Afshar. *Surf. Coat. Technol.,* 339 (2018) 199.
22. M.F. Morks, N.F. Fahim and A.A. Francis. *Surf. Coat. Technol.,* 201 (2006) 282.
23. H. Fan, Y.P. Zhao, S.K. Wang and R.L. Ma. *Mater. Res. Express.,* 6(2019)115090.
24. X.H. Zheng, J. Tan, Q. Zhang, M.Wang and L. Meng. *Surf. Coat. Technol.,* 311 (2017) 151.
25. D.R. Liu, Q. Zhang, Z.B. Qin, Q. Luo, Z. Wu and L. Liu. *Appl. Surf. Sci.,* 363 (2016) 161.
26. C.A. Huang, J.H. Chang, F.Y. Hsu and C.W. Chen. *Surf. Coat. Technol.,* 238 (2014) 87.
27. H. Yang and S.K. Wen. *Int. J. Mach. Tools Manuf.,* 40 (2000) 1065.
28. D. Zhu, W.N. Lei, N.S. Qu and H.Y. Xu. *CIRP. Ann. Manuf. Technol.,* 51 (2002) 173.
29. K.Y. Zhang, J.G. Liu and W. Xiao. *Mater. Lett.,* 193 (2017) 77.
30. S.K. Kumar and K. Biswas. *Surf Coat Technol.* 214 (2013) 8.
31. Y.H. Dong, K.J. Xu and S.G. Liu. *Chin. J. Nonferrous Met.,* 9 (1999) 370.
32. G.Y. Qiao, T.F. Jing and N. Wang. *Electrochim. Acta,* 51 (2005) 181.
33. H. Fan, Y.P. Zhao, J.Jiang, S.K.Wang, W. Shan and R.L.Ma. *Int. J. Electrochem. Sci.*, 15(2020) 2648.
34. H. Fan, Y.P. Zhao, J.Jiang, S.K.Wang, W. Shan and Z.J.Li. *Mater. Trans.,* 61(2020) 795.
35. J. Tan, H. Song and X.H. Zheng. *Surf .Eng.,* 34 (2018) 861.
36. H. Kima, J.G. Kimb and J.W. Parkc. *Precis. Eng.,* 51 (2018) 153.
37. F.F. Xia, W.C. Jia, C.Y. Ma, R. Yang, Y. Wang and M. Potts. *Appl. Surf. Sci.,* 434 (2018) 228.
38. M.S. Rajput, P.M. Pandey and S. Jha. *J. Manuf .Process,* 17 (2015) 98.
39. W. Jiang, L.D. Shen and Q.X. Wang. *J. Alloys. Compd.,* 762 (2018) 115.
40. X. Liu, L.D. Shen and M.B. Qiu. *Surf. Coat. Technol.,* 305 (2016) 231.
41. H. Fan, Y.P. Zhao, J.Jiang, S.K.Wang and H.F. Guo. *Int. J. Adv. Manuf. Technol.,*105 (2019) 4509.
42. Z. J. Tian, D. S. Wang, G. F. Wang, L. D. Shen, Z. D. Liu and Y.H. Huang. *Trans. Nonferrous Met. Soc. China.,* 20 (2010) 1037.
43. W.Z. Huo, L. D. Shen, M.B. Qiu, Z. J. Tian and W. Jiang. *Surf. Coat. Technol.,* 333 (2018) 87.
44. D. Huang, L. Shen and J. Chen. *Trans. Indian. Inst. Met.,* 67 (2014) 351.